

Safe Navigation in Unstructured Environments by Minimizing Uncertainty in Control and Perception

Junwon Seo, Jungwi Mun, and Taekyung Kim
AI Autonomy Technology Center, Agency for Defense Development

Abstract—Uncertainty in control and perception poses challenges for autonomous vehicle navigation in unstructured environments, leading to navigation failures and potential vehicle damage. This paper introduces a framework that minimizes control and perception uncertainty to ensure safe and reliable navigation. The framework consists of two uncertainty-aware models: a learning-based vehicle dynamics model and a self-supervised traversability estimation model. We train a vehicle dynamics model that can quantify the epistemic uncertainty of the model to perform active exploration, resulting in the efficient collection of training data and effective avoidance of uncertain state-action spaces. In addition, we employ meta-learning to train a traversability cost prediction network. The model can be trained with driving data from a variety of types of terrain, and it can online-adapt based on interaction experiences to reduce the aleatoric uncertainty. Integrating the dynamics model and traversability cost prediction model with a sampling-based model predictive controller allows for optimizing trajectories that avoid uncertain terrains and state-action spaces. Experimental results demonstrate that the proposed method reduces uncertainty in prediction and improves stability in autonomous vehicle navigation in unstructured environments.

I. INTRODUCTION

Due to the complex and unpredictable nature of vehicle control and environmental perception, autonomous vehicle navigation in unstructured environments is challenging [1]. Learning-based navigation methods for autonomous, high-speed vehicles in unstructured environments have demonstrated promising results in recent years. The success of fast-moving autonomous vehicles in off-road conditions can be attributed to two crucial factors. The first is learning-based vehicle control [2, 3, 4, 5, 6, 7], and the second is the estimation of off-road terrain traversability [8, 9, 10, 11, 12, 13, 14, 15].

Learning-based vehicle control has become crucial for autonomous vehicles since it facilitates optimal navigation performance while ensuring safety [16, 17, 18, 19]. Recent studies have demonstrated the effectiveness of combining learning-based vehicle dynamics models with model-based controllers [20]. Also, estimating terrain traversability in off-road environments is essential for outdoor navigation. As off-road environments are rife with terrains that may generate uncertain vehicle reactions, failure to identify such uncertainty, which we refer to as *perception failure*, could lead to navigation failure and even severe damage to the vehicle [21, 22, 23, 24, 25]. Recent works present self-supervised

methods for estimating traversability that take into vehicle-terrain interactions pertinent to navigation based on actual driving experiences [26, 27, 28, 29, 30, 31, 32]. They predict traversal costs derived from proprioceptive terrain interaction feedback using exteroceptive sensor measurements.

However, the primary limitation of these learning-based methods of control and perception is that the uncertainty of the model significantly affects the dependability of predictions [33, 34, 35, 30, 36]. Insufficient data to learn vehicle dynamics may result in uncertainty and suboptimal control performance [37, 38]. Self-supervised traversability estimation methods have inherent uncertainty problems since the interaction data only provides supervision for actually traversed regions [21, 36, 39]. Moreover, since the terrain traversability is predicted from a limited sensor configuration (e.g., a sparse LiDAR point cloud) [40, 41, 42, 43, 44], the estimation entails substantial aleatoric uncertainty.

For the safe and reliable navigation of autonomous vehicles in unstructured environments, it is necessary to minimize the uncertainty of predictions regarding both control and perception. The uncertainty-aware navigation can be performed through data exploration during training or online adaptation during deployment [45, 46, 47, 48]. If uncertainty cannot be resolved, reliable navigation can be enforced by preventing vehicles from accessing uncertain state-action spaces or terrain with high levels of uncertainty.

This paper proposes a framework for autonomous vehicle navigation in unstructured environments. To this end, we employ an uncertainty-aware learning-based dynamics model and a self-supervised traversability estimation model. The vehicle dynamics model is trained through a model-based reinforcement learning framework that quantifies epistemic uncertainty. After learning the dynamics model, we generate an uncertainty-aware traversability cost map. Using the self-supervised traversability cost of terrains derived from interaction experiences, the traversability model is capable of online adaptation to minimize uncertainty. We integrate the dynamics model and traversability cost map with a sampling-based model predictive controller. The controller allows for safe navigation by optimizing the trajectory to avoid regions and actions with high uncertainty.

II. METHODS

A. Uncertainty Minimization in Control

We aim to learn a vehicle dynamics model, F , which can minimize uncertainty using active exploration. The system

This work was supported by the Agency For Defense Development Grant funded by the Korean Government (2023).

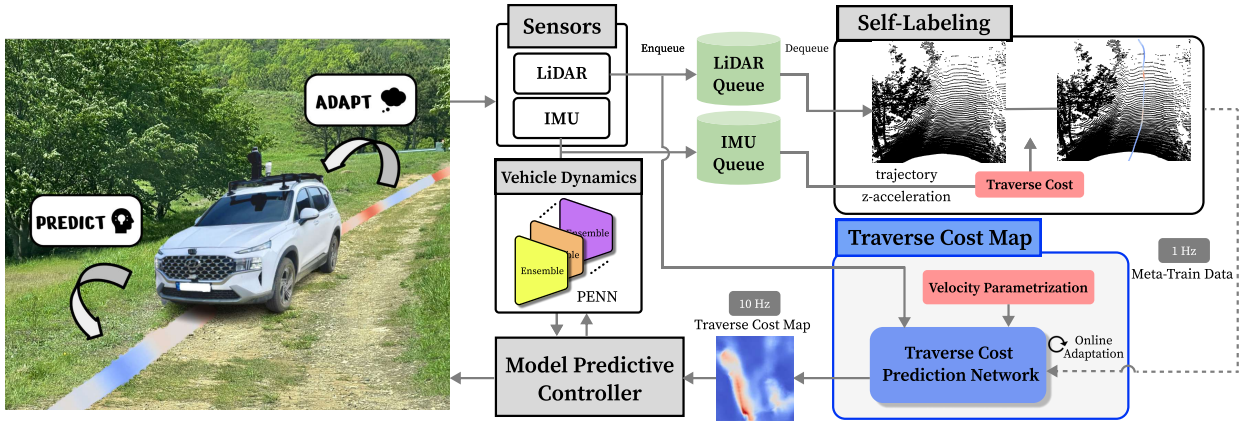


Fig. 1: Diagram of our navigation method that minimizes control and perception uncertainty. While training the dynamics model, active exploration is conducted, which minimizes epistemic uncertainty using a Probabilistic Ensemble Neural Network (PENN). Our traversability cost prediction network reduces aleatoric uncertainty through online adaptation using self-labeled data. Our method enables safe and efficient navigation in unstructured environments by combining uncertainty-minimizing control and perception methods.

dynamics can be defined as $\mathbf{x}_{t+1} = \mathbf{F}(\mathbf{x}_t, \mathbf{u}_t)$ where \mathbf{F} is a nonlinear function, $\mathbf{x}_t \in \mathbb{R}^n$ and $\mathbf{u}_t \in \mathbb{R}^m$ are the observed state vector and applied action input at time t , respectively. Following our previous work [49], we employ Probabilistic Ensemble Neural Network (PENN) to approximate the vehicle dynamics \mathbf{F} [50, 51].

The disagreement between the ensemble model of a state-action pair $D(\mathbf{x}_t, \mathbf{u}_t)$ can be utilized to encourage active exploration in order to collect additional training data. Using a closed-form Jensen-Rényi Divergence [52, 53, 54] that can be calculated in real-time, our previous method [49] demonstrated that the epistemic uncertainty of a given state action pair can be effectively quantified. During the training phase, the vehicle is instructed to collect data with high disagreement so as to accumulate data with high epistemic uncertainty. As additional training data are collected, ensemble models will gradually converge toward increasingly similar predictions, resulting in an eventual reduction in model uncertainty.

For active exploration, Model Predictive Path Integral (MPPI) [2] control is utilized. MPPI is the state-of-the-art sampling-based MPC whose parallelizable structure enables real-time implementation using Graphic Processing Units (GPUs) [55]. Denoting by $U = \{\mathbf{u}_0, \dots, \mathbf{u}_{T-1}\}$ with a fixed time horizon T , the MPPI algorithm seeks an optimal control sequence U^* such that:

$$U^* = \underset{U}{\operatorname{argmin}} \mathbb{E} \left[\phi(\mathbf{x}_T) + \sum_{t=0}^{T-1} \mathcal{L}(\mathbf{x}_t, \mathbf{u}_t) \right], \quad (1)$$

where $\phi(\cdot)$ is a state-dependent terminal cost.

For the active exploration, the model disagreement is added to the controller's objective in order to jointly achieve task-dependent cost optimization and active exploration:

$$\mathcal{L}^{\text{active}}(\mathbf{x}_t, \mathbf{u}_t) = q(\mathbf{x}_t) + \frac{1}{2} \mathbf{u}_t^\top \mathbf{R} \mathbf{u}_t - w_D D(\mathbf{x}_t, \mathbf{u}_t), \quad (2)$$

, where $w_D > 0$ is a weighting constant and $q(\mathbf{x}_t)$ is an arbitrary state-dependent running cost function. The vehicle is encouraged to select behaviors that result in the exploration of ambiguous state-action spaces of the dynamic model.

B. Uncertainty Minimization in Perception

1) *Anomaly Detection for Minimizing Epistemic Uncertainty*: For effective navigation in off-road environments, the traversability of terrain can be determined by interactions between terrain and a vehicle [26, 27]. However, data on such interactions is restricted to traversed regions only, and data collection in non-traversable regions is not feasible. This nature produces overconfident predictions, resulting in navigational failure or even catastrophic outcomes [21].

This issue can be mitigated by employing methods for detecting anomalies [23, 21, 22]. Regions that a vehicle interacted with are designated as positive, on the assumption that terrains with similar geometric properties to those regions are normal and thus less uncertain. Then, we train a binary classifier capable of identifying points that are dissimilar to positive points, indicating high epistemic uncertainty. These regions are designated for avoidance during navigation. The method is described in detail in our previous work [36, 25].

2) *Uncertainty-Aware Traversability Cost Map*: Off-road environments are fraught with bumps and obstacles of varying shapes, despite being in the same terrain class. For safe and effective navigation of a vehicle in off-road terrain, estimating the nuanced traverse cost of the terrain is necessary. A path planner can optimize a trajectory that minimizes disturbances during navigation with the predicted cost. Therefore, we generate dense and continuous traverse cost maps in bird's eye view (BEV) from a single LiDAR point cloud.

The z-axis linear acceleration measured by an Inertial Measurement Unit (IMU) is used to define the traversability that can stabilize navigation, as this component effectively communicates the terrain's bumpiness [28]. In addition, because our controller employs a vehicle dynamics model that is ignorant of vertical motions [56, 7], the definition of traversability based on vertical acceleration can be helpful in preventing control performance losses. Motivated by recent work [32], we define traverse cost using the spectral power of z-acceleration produced by a continuous wavelet transformation.

The network is trained to produce a dense traverse cost

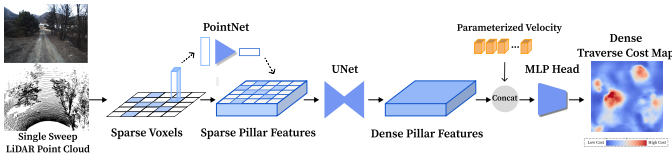


Fig. 2: Overview pipeline of the traversability cost prediction network.

map using a sparse single-sweep LiDAR point cloud in BEV, as shown in Fig. 2. Following PointPillars [57], each point is discretized into sparse voxels with a grid size of 0.2m. Using PointNet [58], each voxel is converted into sparse pillar features. Then, a U-Net [59] structured network, which has an encoder-decoder architecture with skip connections, is employed to generate a dense pillar feature map. It progressively reduces the spatial size of features and captures higher-level semantic information, while the decoder upsamples feature maps to recover spatial information. Then, the dense pillar features are then concatenated with parameterized velocity to produce velocity-conditioned cost maps. The velocity is parameterized with Fourier feature mapping [60] to incorporate vehicle’s velocity into the costmap prediction [32].

Finally, the MLP head predicts the mean μ_i and standard deviation σ_i of the traversability for each pillar i . The network is trained to minimize the Gaussian log-likelihood:

$$\mathcal{L}^{\text{traverse}}(\tau, \theta) = \frac{1}{2} \left(\log(\sigma_i) + \frac{(\mu_i - c_i)^2}{\sigma_i} \right), \quad (3)$$

where τ , c_i , and θ represent a trajectory, the cost of the trajectory that is associated with the pillar i , and model parameter, respectively.

Algorithm 1: Meta Learning of Traverse Cost

Given: θ : \mathcal{D} : Interaction data from various environments;
 M, K : Number of past and future timesteps;
 N : Number of sampled trajectories;
 N_A : Number of the inner gradient steps;
 α, β : Learning rate for inner and outer gradient steps;
 Randomly initialize θ ;

```

for  $i \leftarrow 0$  to maximum iterations do
  for  $j \leftarrow 0$  to  $N - 1$  do
    Sample  $\tau(t - M, t), \tau(t, t + K) \sim \mathcal{D}$ ;
    Self-Label  $\tau(t - M, t)$  and  $\tau(t, t + K)$ ;
     $\theta' \leftarrow \theta$ ;
    for  $k \leftarrow 0$  to  $N_A - 1$  do
       $\theta' \leftarrow \theta' - \alpha \nabla_{\theta'} \mathcal{L}^{\text{traverse}}(\tau(t - M, t), \theta')$ ;
     $\mathcal{L}_j \leftarrow \mathcal{L}^{\text{traverse}}(\tau(t, t + K), \theta')$ 
   $\theta \leftarrow \theta - \beta \nabla_{\theta} \frac{1}{N} \sum_{j=1}^N \mathcal{L}_j$ 

```

3) *Online Adaptation for Minimizing Aleatoric Uncertainty*: A significant degree of aleatoric uncertainty occurs when learning traverse cost from a single-sweep LiDAR point cloud. In real-world off-road environments, there are a variety of terrain types, and the terrain and vehicle properties that influence traversability (e.g., deformability, friction, and roughness) differ according to a number of factors. However, such subtle differences cannot be precisely captured by a LiDAR point cloud. The ground-truth traverse cost of terrain

captured in different environments would vary considerably, while the geometric characteristics of terrain would be comparable. Learning a global traversability model using a large dataset \mathcal{D} of multiple environments leads to high aleatoric uncertainty in estimation.

To resolve this issue, we propose a model that can effectively learn a global traversability model that is capable of quickly adapting to a new environment based on its recent experiences. We use Model-Agnostic Meta-Learning (MAML) [61] for online adaptation of the traversability model. It aims to find the initial parameters of the network so that adaptation with a few gradient descent steps from this initialization leads to effective generalization to current circumstances. By doing so, the model can incorporate driving data collected in various environments for learning traverse cost from geometric properties without confusion.

While terrain properties vary significantly in different environments, we assume that the environment is locally consistent. Consequently, each segment of a trajectory is regarded as a separate *task*, denoted as τ . The traversability model is trained to adapt using the meta-train data of M past timesteps, $\tau(t - M, t)$, to predict the traverse cost of the next K timesteps, $\tau(t, t + K)$, as follows:

$$\begin{aligned} \operatorname{argmin}_{\theta} \quad & \mathbb{E}_{\tau(t-M, t+K) \sim \mathcal{D}} [\mathcal{L}^{\text{traverse}}(\tau(t, t + K), \theta')] \\ \text{s.t.:} \quad & \theta' = \theta - \alpha \nabla_{\theta} \mathcal{L}^{\text{traverse}}(\tau(t - M, t), \theta). \end{aligned} \quad (4)$$

The past M timesteps provide insight on how to adapt the model to precisely predict future trajectories’ traverse costs. As illustrated in Fig.1, the model can online-adapt during the deployment phase using automatically generated meta-train data in a self-supervised manner. Algorithm 1 describes the meta-learning-based training procedure for the global traversability model. The trained global model is applicable in a variety of environments and is even able to adjust to unseen terrain.

III. EXPERIMENTS

Our previous works have demonstrated our methods for minimizing epistemic uncertainty in vehicle dynamics and terrain traversability [49, 36]. Therefore, we concentrate experiments on the integration of methods for autonomous navigation, particularly in terms of online adaptation for traversability (see Section II-B3). Our experiments address the following key questions: **(Q1)** Can our method reduce aleatoric uncertainty for learning traversability cost? **(Q2)** Is our method helpful for safe and stable navigation in unstructured environments? **(Q3)** Can our traversability estimation model online adapt effectively to unknown terrains for navigation?

TABLE I: Validation error of traversability estimation models for real-world driving data. Our method shows a significant margin compared to the baseline.

	Unpaved	Rough	Grassland	Profiled Road	Simulation
<i>Baseline</i>	0.1222	0.0196	0.2460	0.2039	0.7263
<i>w.o. Adaptation</i>	0.0713	0.0171	0.1961	0.1907	0.6668
<i>w. Adaptation</i>	0.0114	0.0015	0.1767	0.1523	0.5725

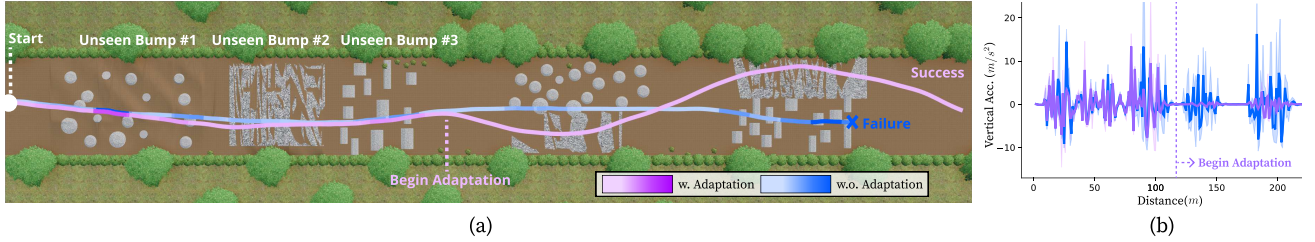


Fig. 3: (a) The off-road race track designed for online adaptation (Q3). The vehicle trajectories are visualized, and the colors of the lines illustrate the rotational impacts exerted on the vehicle. (b) Vertical acceleration of the vehicle during navigation. By conducting online adaptation, the vehicle can plan paths that can minimize impacts exerted on the vehicle, leading to stable navigation in off-road.

A. Minimizing Aleatoric Uncertainty of Traversability Cost

Experimental Setup We quantitatively evaluate our meta-learning method for traversability cost prediction (Q1). We collect driving data in various types of terrain with our vehicle (See Fig. 1) equipped with OS1-128 LiDAR and IMU. Also, the driving data is obtained in a simulation environment consisting of randomly patterned rough terrain and bumps. Approximately five hours of driving data are utilized to train the network. For comparison, a global model (*Baseline*) is simply trained without adaptation.

Experimental Result The Table I provides the Mean Square Error (MSE) between the ground-truth traversability and the predicted traversability cost. In every category, our method produces superior results compared to the baseline. It means the non-meta-learned baseline failed to converge due to high aleatoric uncertainty in ground-truth traversability gathered in various terrains, whereas our meta-learned model can converge well by incorporating such uncertainty during training. Our method even shows better performance without adaptation during the inference (*w.o. Adaptation*), meaning that it finds a better initial parameter. Moreover, the performance improves as the model adapts using the meta-train data derived from past interaction experiences (*w. Adaptation*).

B. Safe Navigation in Unstructured Environment

Experimental Setup We evaluate Q2-Q3 using a high-fidelity vehicle dynamics simulator - IPG CarMaker. For all experiments, navigation is performed using only local traversability maps generated from LiDAR point clouds, with no prior knowledge or global map of the environments. For each method, navigation is performed 15 times.

A realistic off-road environment is designed with large bumps and randomly patterned rough terrain (see Fig. 4) to conduct navigation with traversability maps produced by various methods (Q2). Traversability maps are produced from our method with and without online adaptation, an elevation-map based method (*Elevation Based*) [62, 63], and a slope-based method (*Slope Based*) [64, 65].

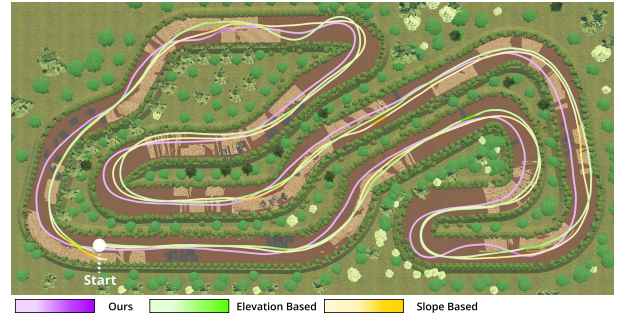


Fig. 4: The off-road race track designed in the IPG CarMaker simulator for navigation experiments. The vehicle trajectory is displayed.

An additional off-road environment is designed with several unknown types of bumps (see Fig. 3), to validate that our model is capable of online-adapting to unknown terrains (Q3), which eventually results in safe navigation. The vehicle begins to adapt after experiencing three unseen types of bumps. This allows the vehicle to effectively optimize trajectories that minimize perturbation when re-encountering the bumps.

Based on our prior work [56], we formulate a simple running cost function $q(\mathbf{x}_t)$ of the controller, which is designed to minimize the traversability cost of a trajectory while maintaining the 30 km/h target speed:

$$q(\mathbf{x}_t) = \alpha_1 \text{Track}(\mathbf{x}_t) + \alpha_2 \text{Stable}(\mathbf{x}_t) + \alpha_3 \text{Speed}(\mathbf{x}_t), \quad (5)$$

where $\text{Track}(\mathbf{x}_t)$ and $\text{Stable}(\mathbf{x}_t)$ are assigned based on the local traversability map. $\text{Track}(\mathbf{x}_t)$ imposes a significant penalty based on (Sec. II-B1) and $\text{Stable}(\mathbf{x}_t)$ is based on the traversability cost map generated by our method (Sec. II-B2).

Experimental Results The trajectories taken during navigation are shown in Fig. 4. Compared to other rule-based methods, the vehicle using our traversability map navigates along trajectories that minimize disturbances. Table. II shows the average values of the vehicle’s vertical and angular motions. It shows that our map of traversability can assist in stabilizing the vehicle during off-road navigation.

Fig. 3 shows the navigation results in the scene designed for evaluating online-adaptation. The vehicle experiences unseen bumps and effectively adapts the model to incorporate the experience. After adaptation, the controller determines to avoid difficult bumps, whereas the vehicle without adaptation fails to avoid them, resulting in a rollover. By beginning to online-adapt the network, the vehicle is capable of reducing the impact exerted on it, while the vehicle not conducting adaptation continues to experience enormous impacts.

TABLE II: The average and maximum motions of the vehicle across all trials.

Method	Success Rate	Vertical Vel. [m/s]		Vertical Acc. [m/s ²]		Roll Acc. [rad/s ²]		Pitch Acc. [rad/s ²]	
		Mean	Max	Mean	Max	Mean	Max	Mean	Max
Elevation Based	7 / 15	0.152	2.766	1.254	40.108	1.287	54.783	1.177	34.029
Slope Based	6 / 15	0.128	1.846	0.999	30.481	1.018	38.910	0.953	26.822
Ours(w.o. Adaptation)	14 / 15	0.109	1.690	0.868	27.948	0.899	36.022	0.878	27.046
Ours(w. Adaptation)	15 / 15	0.106	1.591	0.854	25.686	0.892	32.217	0.849	22.079

REFERENCES

- [1] P. Borges, T. Peynot, S. Liang, B. Arain, M. Wildie, M. Minareci, S. Lichman, G. Samvedi, I. Sa, N. Hudson *et al.*, “A survey on terrain traversability analysis for autonomous ground vehicles: Methods, sensors, and challenges,” *Field Robotics*, vol. 2, no. 1, pp. 1567–1627, 2022. [i](#)
- [2] G. Williams, N. Wagener, B. Goldfain, P. Drews, J. M. Rehg, B. Boots, and E. A. Theodorou, “Information theoretic MPC for model-based reinforcement learning,” in *IEEE International Conference on Robotics and Automation (ICRA)*, 2017, pp. 1714–1721. [i](#), [ii](#)
- [3] M. Lutter, C. Ritter, and J. Peters, “Deep Lagrangian Networks: Using Physics as Model Prior for Deep Learning,” in *International Conference on Learning Representations (ICLR)*, 2019. [i](#)
- [4] A. Nagabandi, K. Konolige, S. Levine, and V. Kumar, “Deep dynamics models for learning dexterous manipulation,” in *Conference on Robot Learning (CoRL)*, 2019, pp. 1101–1112. [i](#)
- [5] Y. Yang, K. Caluwaerts, A. Iscen, T. Zhang, J. Tan, and V. Sindhwani, “Data Efficient Reinforcement Learning for Legged Robots,” in *Conference on Robot Learning (CoRL)*, 2019, pp. 1–10. [i](#)
- [6] D. Shah, A. Sridhar, A. Bhorkar, N. Hirose, and S. Levine, “GNM: A General Navigation Model to Drive Any Robot,” in *arXiv*, 2022. [Online]. Available: <https://arxiv.org/abs/2210.03370> [i](#)
- [7] T. Kim, H. Lee, and W. Lee, “Physics Embedded Neural Network Vehicle Model and Applications in Risk-Aware Autonomous Driving Using Latent Features,” in *IEEE/RSJ International Conference on Intelligent Robots and Systems (IROS)*, 2022, pp. 4182–4189. [i](#), [ii](#)
- [8] H. Lee, K. Kwak, and S. Jo, “An incremental non-parametric bayesian clustering-based traversable region detection method,” *Autonomous Robots*, vol. 41, pp. 795–810, 2017. [i](#)
- [9] J. Ahtinen, T. Stoyanov, and J. Saarinen, “Normal distributions transform traversability maps: Lidar-only approach for traversability mapping in outdoor environments,” *Journal of Field Robotics*, vol. 34, no. 3, pp. 600–621, 2017. [i](#)
- [10] C. Sevastopoulos and S. Konstantopoulos, “A survey of traversability estimation for mobile robots,” *IEEE Access*, vol. 10, pp. 96 331–96 347, 2022. [i](#)
- [11] T. Guan, D. Kothandaraman, R. Chandra, A. J. Sathiamoorthy, K. Weerakoon, and D. Manocha, “Ganav: Efficient terrain segmentation for robot navigation in unstructured outdoor environments,” *IEEE Robotics and Automation Letters*, vol. 7, no. 3, pp. 8138–8145, 2022. [i](#)
- [12] B. Gao, S. Hu, X. Zhao, and H. Zhao, “Fine-grained off-road semantic segmentation and mapping via contrastive learning,” in *IEEE/RSJ International Conference on Intelligent Robots and Systems (IROS)*, 2021, pp. 5950–5957. [i](#)
- [13] J. Frey, D. Hoeller, S. Khattak, and M. Hutter, “Locomotion policy guided traversability learning using volumetric representations of complex environments,” in *IEEE/RSJ International Conference on Intelligent Robots and Systems (IROS)*, 2022, pp. 5722–5729. [i](#)
- [14] A. J. Sathiamoorthy, K. Weerakoon, T. Guan, J. Liang, and D. Manocha, “Terrapn: Unstructured terrain navigation using online self-supervised learning,” in *IEEE/RSJ International Conference on Intelligent Robots and Systems (IROS)*, 2022, pp. 7197–7204. [i](#)
- [15] K. Weerakoon, A. J. Sathiamoorthy, U. Patel, and D. Manocha, “Terp: Reliable planning in uneven outdoor environments using deep reinforcement learning,” in *International Conference on Robotics and Automation (ICRA)*, 2022, pp. 9447–9453. [i](#)
- [16] J. Kabzan, L. Hewing, A. Liniger, and M. N. Zeilinger, “Learning-based model predictive control for autonomous racing,” *IEEE Robotics and Automation Letters*, vol. 4, no. 4, pp. 3363–3370, 2019. [i](#)
- [17] P. Wu, A. Escontrela, D. Hafner, K. Goldberg, and P. Abbeel, “DayDreamer: World Models for Physical Robot Learning,” in *Conference on Robot Learning (CoRL)*, 2022. [i](#)
- [18] S. J. Wang, S. Triest, W. Wang, S. Scherer, and A. Johnson, “Rough terrain navigation using divergence constrained model-based reinforcement learning,” in *Conference on Robot Learning (CoRL)*, 2021. [i](#)
- [19] T. Kim, H. Lee, S. Hong, and W. Lee, “TOAST: Trajectory Optimization and Simultaneous Tracking Using Shared Neural Network Dynamics,” *IEEE Robotics and Automation Letters*, vol. 7, no. 4, pp. 9747–9754, 2022. [i](#)
- [20] G. Kahn, P. Abbeel, and S. Levine, “Badgr: An autonomous self-supervised learning-based navigation system,” *IEEE Robotics and Automation Letters*, vol. 6, no. 2, pp. 1312–1319, 2021. [i](#)
- [21] L. Wellhausen, R. Ranftl, and M. Hutter, “Safe robot navigation via multi-modal anomaly detection,” *IEEE Robotics and Automation Letters*, vol. 5, no. 2, pp. 1326–1333, 2020. [i](#), [ii](#)
- [22] T. Ji, S. T. Vuppala, G. Chowdhary, and K. Driggs-Campbell, “Multi-modal anomaly detection for unstructured and uncertain environments,” in *Conference on Robot Learning (CoRL)*, 2021, pp. 1443–1455. [i](#), [ii](#)
- [23] H. R. Kerner, D. F. Wellington, K. L. Wagstaff, J. F. Bell, C. Kwan, and H. B. Amor, “Novelty detection for multispectral images with application to planetary exploration,” in *Proceedings of the AAAI conference on artificial intelligence*, vol. 33, no. 01, 2019, pp. 9484–9491. [i](#), [ii](#)
- [24] T. Ji, A. N. Sivakumar, G. Chowdhary, and K. Driggs-Campbell, “Proactive anomaly detection for robot navigation with multi-sensor fusion,” *IEEE Robotics and Automation Letters*, vol. 7, no. 2, pp. 4975–4982, 2022. [i](#)

- [25] J. Seo, S. Sim, and I. Shim, "Learning off-road terrain traversability with self-supervisions only," *IEEE Robotics and Automation Letters*, vol. 8, no. 8, pp. 4617–4624, 2023. [i](#), [ii](#)
- [26] L. Wellhausen, A. Dosovitskiy, R. Ranftl, K. Walas, C. Cadena, and M. Hutter, "Where should i walk? predicting terrain properties from images via self-supervised learning," *IEEE Robotics and Automation Letters*, vol. 4, no. 2, pp. 1509–1516, 2019. [i](#), [ii](#)
- [27] J. Zürn, W. Burgard, and A. Valada, "Self-supervised visual terrain classification from unsupervised acoustic feature learning," *IEEE Transactions on Robotics*, vol. 37, no. 2, pp. 466–481, 2020. [i](#), [ii](#)
- [28] M. A. Bekhti, Y. Kobayashi, and K. Matsumura, "Terrain traversability analysis using multi-sensor data correlation by a mobile robot," in *IEEE/SICE International Symposium on System Integration*, 2014, pp. 615–620. [i](#), [ii](#)
- [29] C. A. Brooks and K. D. Iagnemma, "Self-supervised classification for planetary rover terrain sensing," in *IEEE Aerospace Conference (AERO)*, 2007, pp. 1–9. [i](#)
- [30] X. Cai, M. Everett, J. Fink, and J. P. How, "Risk-aware off-road navigation via a learned speed distribution map," in *IEEE/RSJ International Conference on Intelligent Robots and Systems (IROS)*, 2022, pp. 2931–2937. [i](#)
- [31] M. V. Gasparino, A. N. Sivakumar, Y. Liu, A. E. Velasquez, V. A. Higuti, J. Rogers, H. Tran, and G. Chowdhary, "Wayfast: Navigation with predictive traversability in the field," *IEEE Robotics and Automation Letters*, vol. 7, no. 4, pp. 10 651–10 658, 2022. [i](#)
- [32] M. Guaman Castro, S. Triest, W. Wang, J. M. Gregory, F. Sanchez, J. G. Rogers III, and S. Scherer, "How does it feel? self-supervised costmap learning for off-road vehicle traversability," in *IEEE International Conference on Robotics and Automation (ICRA)*, 2023. [i](#), [ii](#), [iii](#)
- [33] D. Nguyen-Tuong and J. Peters, "Model learning for robot control: a survey," *Cognitive Processing*, vol. 12, no. 4, pp. 319–340, 2011. [i](#)
- [34] S. Palazzo, D. C. Guastella, L. Cantelli, P. Spadaro, F. Rundo, G. Muscato, D. Giordano, and C. Spampinato, "Domain adaptation for outdoor robot traversability estimation from rgb data with safety-preserving loss," in *IEEE/RSJ International Conference on Intelligent Robots and Systems (IROS)*. IEEE, 2020, pp. 10 014–10 021. [i](#)
- [35] D. D. Fan, A.-A. Agha-Mohammadi, and E. A. Theodorou, "Learning risk-aware costmaps for traversability in challenging environments," *IEEE Robotics and Automation Letters*, vol. 7, no. 1, pp. 279–286, 2021. [i](#)
- [36] J. Seo, T. Kim, K. Kwak, J. Min, and I. Shim, "Scate: A scalable framework for self-supervised traversability estimation in unstructured environments," *IEEE Robotics and Automation Letters*, vol. 8, no. 2, pp. 888–895, 2023. [i](#), [ii](#), [iii](#)
- [37] G. Kahn, A. Villaflor, V. Pong, P. Abbeel, and S. Levine, "Uncertainty-Aware Reinforcement Learning for Collision Avoidance," in *arXiv preprint arXiv:1702.01182*, 2017. [i](#)
- [38] A. Parsi, A. Iannelli, and R. S. Smith, "Active exploration in adaptive model predictive control," in *IEEE Conference on Decision and Control (CDC)*, 2020, pp. 6186–6191. [i](#)
- [39] J. Frey, M. Mattamala, N. Chebrolu, C. Cadena, M. Fallon, and M. Hutter, "Fast traversability estimation for wild visual navigation," in *Robotics: Science and Systems (RSS)*, 2023. [i](#)
- [40] J. Fei, K. Peng, P. Heidenreich, F. Bieder, and C. Stiller, "Pillarsegnet: Pillar-based semantic grid map estimation using sparse lidar data," in *IEEE Intelligent Vehicles Symposium (IV)*, 2021, pp. 838–844. [i](#)
- [41] R. Cheng, C. Agia, Y. Ren, X. Li, and L. Bingbing, "S3cnet: A sparse semantic scene completion network for lidar point clouds," in *Conference on Robot Learning (CoRL)*, 2021, pp. 2148–2161. [i](#)
- [42] Y. Han, J. Banfi, and M. Campbell, "Planning paths through unknown space by imagining what lies therein," in *Conference on Robot Learning (CoRL)*, 2021, pp. 905–914. [i](#)
- [43] K. Peng, J. Fei, K. Yang, A. Roitberg, J. Zhang, F. Bieder, P. Heidenreich, C. Stiller, and R. Stiefelhagen, "Mass: Multi-attentional semantic segmentation of lidar data for dense top-view understanding," *IEEE Transactions on Intelligent Transportation Systems*, vol. 23, no. 9, pp. 15 824–15 840, 2022. [i](#)
- [44] A. Shaban, X. Meng, J. Lee, B. Boots, and D. Fox, "Semantic terrain classification for off-road autonomous driving," in *Conference on Robot Learning (CoRL)*, 2022, pp. 619–629. [i](#)
- [45] A. Nagabandi, I. Clavera, S. Liu, R. S. Fearing, P. Abbeel, S. Levine, and C. Finn, "Learning to adapt in dynamic, real-world environments through meta-reinforcement learning," in *International Conference on Learning Representations (ICLR)*, 2018. [i](#)
- [46] S. Banerjee, J. Harrison, P. M. Furlong, and M. Pavone, "Adaptive meta-learning for identification of rover-terrain dynamics," in *Int. Symp. on Artificial Intelligence, Robotics and Automation in Space*, 2020. [i](#)
- [47] S. M. Richards, N. Azizan, J.-J. E. Slotine, and M. Pavone, "Adaptive-control-oriented meta-learning for nonlinear systems," in *Robotics: Science and Systems (RSS)*, 2021. [i](#)
- [48] M. Visca, R. Powell, Y. Gao, and S. Fallah, "Deep meta-learning energy-aware path planner for unmanned ground vehicles in unknown terrains," *IEEE Access*, vol. 10, pp. 30 055–30 068, 2022. [i](#)
- [49] T. Kim, J. Mun, J. Seo, B. Kim, and S. Hong, "Bridging active exploration and uncertainty-aware deployment using probabilistic ensemble neural network dynamics," *Robotics: Science and Systems (RSS)*, 2023. [ii](#), [iii](#)
- [50] K. Chua, R. Calandra, R. McAllister, and S. Levine, "Deep Reinforcement Learning in a Handful of Trials using Probabilistic Dynamics Models," in *Neural Infor-*

- mation Processing Systems (*NeurIPS*), 2018. [ii](#)
- [51] J. Buckman, D. Hafner, G. Tucker, E. Brevdo, and H. Lee, “Sample-Efficient Reinforcement Learning with Stochastic Ensemble Value Expansion,” in *Neural Information Processing Systems (NeurIPS)*, 2018. [ii](#)
- [52] A. Rényi, “On measures of entropy and information,” in *Proceedings of the Fourth Berkeley Symposium on Mathematical Statistics and Probability*, 1961, pp. 547–562. [ii](#)
- [53] F. Wang, T. Syeda-Mahmood, B. C. Vemuri, D. Beymer, and A. Rangarajan, “Closed-Form Jensen-Renyi Divergence for Mixture of Gaussians and Applications to Group-Wise Shape Registration,” in *International Conference on Medical Image Computing and Computer-Assisted Intervention (MICCAI)*, vol. 5761, 2009, pp. 648–655. [ii](#)
- [54] P. Shyam, W. Jaśkowski, and F. Gomez, “Model-based active exploration,” in *International Conference on Machine Learning (ICML)*, 2019, pp. 5779–5788. [ii](#)
- [55] G. Williams, P. Drews, B. Goldfain, J. M. Rehg, and E. A. Theodorou, “Information-theoretic model predictive control: Theory and applications to autonomous driving,” *IEEE Transactions on Robotics*, vol. 34, no. 6, pp. 1603–1622, 2018. [ii](#)
- [56] T. Kim, G. Park, K. Kwak, J. Bae, and W. Lee, “Smooth Model Predictive Path Integral Control Without Smoothing,” *IEEE Robotics and Automation Letters*, vol. 7, no. 4, pp. 10 406–10 413, 2022. [ii](#), [iv](#)
- [57] A. H. Lang, S. Vora, H. Caesar, L. Zhou, J. Yang, and O. Beijbom, “Pointpillars: Fast encoders for object detection from point clouds,” in *Proceedings of the IEEE/CVF Conference on Computer Vision and Pattern Recognition (CVPR)*, 2019, pp. 12 697–12 705. [iii](#)
- [58] C. R. Qi, H. Su, K. Mo, and L. J. Guibas, “Pointnet: Deep learning on point sets for 3d classification and segmentation,” in *Proceedings of the IEEE Conference on Computer Vision and Pattern Recognition (CVPR)*, 2017, pp. 652–660. [iii](#)
- [59] O. Ronneberger, P. Fischer, and T. Brox, “U-net: Convolutional networks for biomedical image segmentation,” in *Medical Image Computing and Computer-Assisted Intervention (MICCAI)*. Springer, 2015, pp. 234–241. [iii](#)
- [60] M. Tancik, P. Srinivasan, B. Mildenhall, S. Fridovich-Keil, N. Raghavan, U. Singhal, R. Ramamoorthi, J. Barron, and R. Ng, “Fourier features let networks learn high frequency functions in low dimensional domains,” *Neural Information Processing Systems (NeurIPS)*, vol. 33, pp. 7537–7547, 2020. [iii](#)
- [61] C. Finn, P. Abbeel, and S. Levine, “Model-agnostic meta-learning for fast adaptation of deep networks,” in *International Conference on Machine Learning (ICML)*, 2017, pp. 1126–1135. [iii](#)
- [62] P. Fankhauser, M. Bloesch, C. Gehring, M. Hutter, and R. Siegwart, “Robot-centric elevation mapping with uncertainty estimates,” in *Mobile Service Robotics*. World Scientific, 2014, pp. 433–440. [iv](#)
- [63] T. Miki, L. Wellhausen, R. Grandia, F. Jenelten, T. Homberger, and M. Hutter, “Elevation mapping for locomotion and navigation using gpu,” in *IEEE/RSJ International Conference on Intelligent Robots and Systems (IROS)*, 2022, pp. 2273–2280. [iv](#)
- [64] J. Sock, J. Kim, J. Min, and K. Kwak, “Probabilistic traversability map generation using 3d-lidar and camera,” in *IEEE International Conference on Robotics and Automation (ICRA)*, 2016, pp. 5631–5637. [iv](#)
- [65] J. Kim, J. Min, K. Kwak, and K. Bae, “Traversable region detection based on a lateral slope feature for autonomous driving of ugv,” *Journal of Institute of Control, Robotics and Systems*, vol. 23, no. 2, pp. 67–75, 2017. [iv](#)